Int J Adv Manuf Technol (2015) 81:1723–1732
DOI 10.1007/s00170-015-7219-7

ORIGINAL ARTICLE

A theoretical analysis and experimental verification of a laser drilling process for a ceramic substrate

Ming-Fei Chen[1] · **Wen-Tse Hsiao**[2] · **Ming-Cheng Wang**[1] · **Kai-Yu Yang**[1] · **Ying-Fang Chen**[1]

Received: 15 October 2014 / Accepted: 26 April 2015 / Published online: 27 May 2015

Abstract This paper reports theoretical and experimental methods for drilling alumina ceramic substrates by using a nanosecond-pulsed ultraviolet laser. A physical model was established using ANSYS parameter design language finite element software. The influence of laser parameters, such as laser fluence, number of pulses and its duration, and frequency, on morphology—depth, diameter, taper, and temperature distribution—was investigated using three-dimensional confocal laser scanning microscopy. Simulation and experimental results reveal that higher laser fluence and number of pulses produces larger drilling depths and diameters. Laser fluence, pulse duration, frequency, and pulse number of 5.10 J/cm^2, 1000 μs, 20 kHz, and >9, respectively, can successfully drill through the alumina ceramic substrate. Pulse duration between 3 and 8 ms yielded the smallest hole taper.

Keywords Al_2O_3 ceramic · Nanosecond-pulsed ultraviolet laser · Temperature distribution

1 Introduction

Advances in ceramic technology have led to its application in various fields, such as automotive, telecommunication, power electronics, and sensor systems. They exhibit desirable characteristics, such as strong insulation, high thermal efficiency, low warping and thermal expansion coefficients, low material cost, and ease of manufacturing. Most high-efficiency LED products use ceramic materials as thermal slugs.

Several nontraditional fabrication methods, such as chemical wet etching, electrical discharge machining, electrochemical machining, electrochemical drilling, and jet electrolytic drilling [1], have been explored for fabricating compact and multifunctional ceramic devices, and laser machining is increasingly being used. The interaction between the ceramic material and the laser energy melts or vaporizes the ceramic material surface, which removes material; temperature distribution is therefore crucial in this process. Appropriate parameters produce the optimal pore diameter and reduce fabrication costs. Theoretical and experimental studies have explored the influence of laser machining parameters on ceramic morphology; appropriate parameters produce the optimal pore diameter and reduce fabrication costs. Bandyopadhyay et al. [2] presented a 400-W Nd:YAG laser drilling mechanism for 4- and 8-mm-thick Ti–6Al–4V alloys for aerospace applications and analyzed the parameters influencing laser drilling; their experimental results revealed that pulse repetition frequency and laser energy were the most influential. Hanon et al. [3] used ANSYS finite element analysis to simulate temperature distribution in laser alumina ceramic plates. They studied the effect of laser peak power and pulse duration on drilling. Yang et al. [4] studied YAG laser cutting for multiple glass layers and showed that if the upper glass layer temperature is greater than that of the lower layer, the upper layer cutting quality is poor. Samant et al. [5] used the Taguchi method to determine the optimal Nd:YAG laser parameters, including pulse width, pulse frequency, and the scanning speed for treating the alumina ceramic surface. Samant et al. [6] investigated laser machining of ceramic materials and demonstrated that lasers are

✉ Wen-Tse Hsiao
wentse@itrc.narl.org.tw

[1] Department of Mechatronics Engineering, National Changhua University of Education, Changhua 50007, Taiwan

[2] Instrument Technology Research Center, National Applied Research Laboratories, 20 R&D Road VI, Hsinchu Science Park, Hsinchu 30076, Taiwan

highly efficient in processing ceramic materials and do not entail tool wear and workpiece clamping difficulties. Bharatish et al. [7] used the Taguchi method and gray relational analysis to determine the optimal CO_2 nanosecond laser drilling parameters for alumina ceramic materials and identified frequency, power, scanning speed, and diameter as the influencing parameters. Studies have shown that pulse frequency has the strongest effect on the taper and diameter of drill holes. Ren et al. [8] reported the theoretical and experimental results of drilling titanium sheets by using a nanosecond-pulsed Nd:YAG laser; the numerically simulated values were smaller than the experimental values, possibly because the defocusing, plasma, and melting phenomena affect laser drilling, and these behaviors are difficult to simulate. Shukla and Lawrence [9] proposed a fiber and CO_2 laser surface treatment of Si_3N_4 engineering ceramics and showed that laser surface treatment using near-infrared (NIR) fiber lasing is more effective for Si_3N_4 engineering ceramics. Ganguly et al. [10] used the Taguchi method and gray relational analysis method to determine the optimal parameters for laser microdrilling zirconium oxide substrates, and optimizing the parameters improved the hole taper and the width of the heat affect zone. Kibria et al. [11] reported various laser defocusing conditions for treating alumina ceramic surfaces through laser microturning; they used multiobject optimization to obtain minimal surface roughness and depth deviation. After laser surface treatment of the cylindrical-shaped alumina ceramic, surface roughness decreased with an increasing number of laser scan passes for all defocusing positions; however, depth deviation increased with an increasing number of passes. Adelmann and Hellmann [12] used a single-mode fiber laser for drilling alumina and aluminum nitride with thicknesses ranging from 0.25 to 1.5 mm; focus positions were controlled to obtain drill holes with small taper diameters. The drilling times for both materials and all thicknesses were <1 ms, with 0.1 ms for 0.25 mm alumina being the shortest.

The present study theoretically and experimentally investigated the nanosecond-pulsed ultraviolet laser drilling characteristics of alumina ceramic substrates; various parameters, such as laser fluence, pulse, and frequency, and number of pulses, were analyzed. A physical model for laser drilling ceramic substrates was established using ANSYS parameter design language (APDL) finite element software. After laser drilling, the depth, diameter, and taper of the drilled holes were evaluated using a three-dimensional (3D) confocal laser scanning microscope.

2 Theoretical analysis and simulation

In this paper, the laser source is considered a Gaussian energy source. APDL is used to establish a mathematical simulation model for the laser drilling of a ceramic substrate. Subsequently, temperature distribution and thermal characteristics of drilling are determined. Finally, optimal lasing parameters that enhance drilling efficiency are obtained.

2.1 Finite element thermal analysis

The heat density generated by laser power is described using the Gaussian distribution function displayed in Eqs. (1) and (2) [13]:

$$I(x,y,z,t) = \frac{2\alpha P_{\mathrm{p}}}{\pi r^2}\exp\left[-\frac{2(x^2+y^2)}{r^2}\right]\delta(t) \tag{1}$$

$$r = \frac{d}{2}\left[1+\left(M^2\times\frac{4\lambda(Z_{\mathrm{m}}+f_{\mathrm{c}})}{\pi d^2}\right)\right] \tag{2}$$

where α is the material absorption coefficient; r is the radius of the effective light beam, which varies with the depth of the drilling hole; $\delta(t)$ is a pulse function; d is the diameter of the laser beam; f_{c} is the focal length of the focusing lens; Z_{m} is the ceramic melting depth; λ is the laser wavelength; and P_{P} is the instantaneous laser power, which is obtained using Eq. (3):

$$P_{\mathrm{p}} = \frac{P_{\mathrm{a}}}{\mathrm{PRF}\times\Delta t} \tag{3}$$

where P_{a} is the average laser power, PRF represents the pulse repetition frequency, and Δt is the pulse width. For evaluating temperature distribution, the 3D heat conduction equation is expressed as follows [14–17]:

$$\frac{\partial T}{\partial t} = \frac{k}{\rho c_{\mathrm{p}}}\left(\frac{\partial^2 T}{\partial x^2}+\frac{\partial^2 T}{\partial y^2}+\frac{\partial^2 T}{\partial z^2}+\frac{q_{\mathrm{v}}}{k}\right) \tag{4}$$

However, the laser drilling process is considered fully axisymmetric along the laser beam axis. Therefore, the heat conduction equation is reduced to Eq. (5):

$$\frac{\partial T}{\partial t} = \frac{k}{\rho c_p}\left(\frac{\partial^2 T}{\partial x^2}+\frac{\partial^2 T}{\partial y^2}+\frac{q_v}{k}\right) \tag{5}$$

where T is the temperature; k, ρ, and c_{p} are the temperature-dependent thermal conductivity, density, and specific heat, respectively; q_{v} is the intensity of the heating source; and x, y, and z are the coordinate axes, as shown in Fig. 1.

2.2 Finite element thermal analysis of the ceramic substrate

The laser drilling geometry is created and meshed using the APDL function of the finite element analysis software ANSYS. The finite element thermal analysis of the ceramic substrate is in terms of transient heat conduction. The temperature distribution of ceramic drilling varies with time and boundary conditions. Figure 1 presents the flow chart of the analysis.

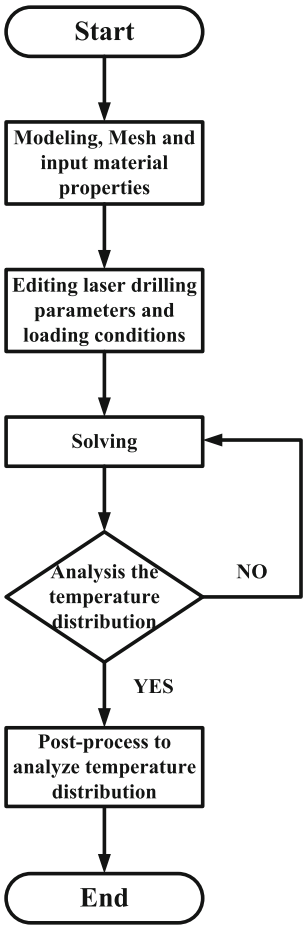

Fig. 1 Flowchart for the thermal analysis

First, the geometric model is meshed using PLAN70 thermal brick elements. Next, the physical parameters of the material, such as thermal conductivity, specific heat, density, and absorption rate, are set. The following conditions are assumed for simulating laser drilling of alumina substrates:

(a) The laser distribution of the beam intensity is a TEM_{00} Gaussian mode.
(b) The material is homogeneous and exhibits isotropic heat transfer characteristics.
(c) The laser-produced plasma phenomenon is ignored.
(d) The laser-generated reflection within the hole is negligible.

Table 1 Specifications of the laser system

Laser source	Pulsed ultraviolet
Wavelength (nm)	355
Pulse width (ns)	14 ns @ 20 kHz
Laser mode	TEM_{00} (M^2<1.2)
Focal length	74.5 mm
Maximum output power (W)	2.6 @ 20 kHz

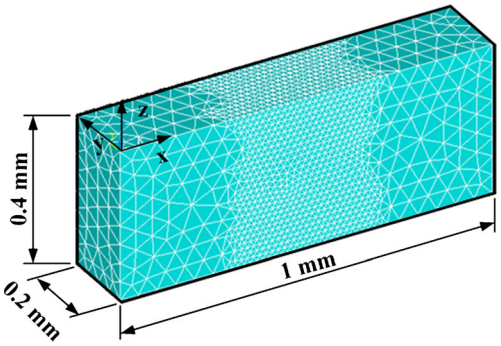

Fig. 2 Analysis model in three dimensions

(e) A laser beam that acts at the material surface is affected by absorption, reflectivity, transmission, and surface roughness of the material. However, for simplification, only absorption and reflectivity are considered.

2.3 Material absorption

In this study, the substrate is a ceramic; therefore, transmittance is zero. The thermal analysis is affected only by the heat absorption and reflectivity of the substrate; therefore, prior to thermal simulation, the absorption and reflectivity of the ceramic is measured. Equation (6) shows the relationship between absorption, reflectivity, and transmittance.

$$A = 1-R-T \tag{6}$$

where A, R, and T, respectively, represent absorption, reflectivity, and transmittance. The reflectivity spectra were measured using a UV–Vis–NIR spectrophotometer (V-670, Jasco Inc.). Using Eq. (6), the absorption percentage for ceramics for wavelengths at 355 nm is 10.17 %.

3 Experimental equipment, parameters, and materials

In the experiments, the alumina specimens with a thickness of 0.4 mm were used. UV laser processing systems with maximal laser output power and laser wavelength of 2.6 W and 355 nm, respectively, were designed and developed; the other

Table 2 Specifications of the Al_2O_3 ceramic material

Physical properties	Material (Al_2O_3)
Melting temperature (°C)	2053
Vaporization temperature (°C)	3503
Density (kg/m^3)	3900
Heat conduction (W/mK)	28
Specific heat (J/kgK)	880

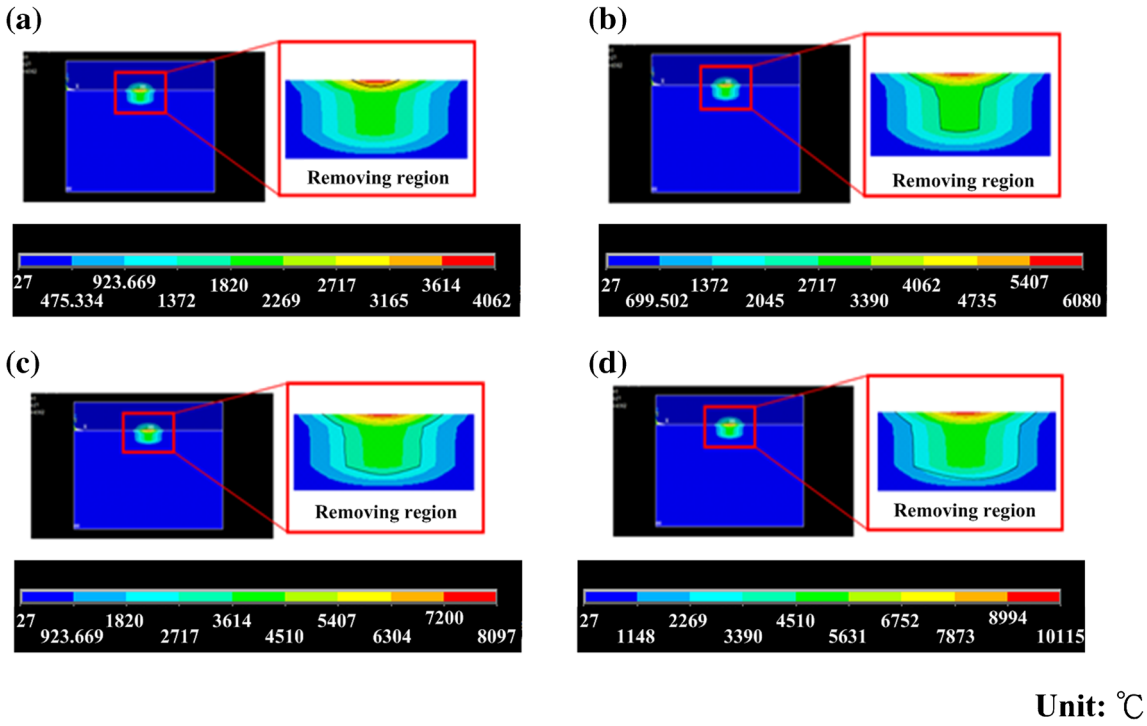

Fig. 3 Simulation results for different values of laser fluence: **a** 2.55 J/cm^2, **b** 3.82 J/cm^2, **c** 5.10 J/cm^2, and **d** 6.37 J/cm^2

parameters are listed in Table 1. Laser output pulse mode was used, and the experimental parameters were laser power, number of pulses, and pulse duration. Laser fluence, number of pulses, and laser pulse duration were varied from 2.55 to 6.37 J/cm^2, 1 to 10, and 10 to 100 ms, respectively. The laser machining focus position was located on the ceramic surface. The specimens were placed on the platform of the laser processing system, and the focus position was adjusted through *z*-axis adjustment; the processing platform then remained stationary. A power meter was used to correct the average laser power. The experiments were performed at room temperature without using assistance gas. A 3D confocal microscope and an optical microscope measured the diameter and the depth of the drilled holes.

4 Simulation results and experimental verification

4.1 Physical parameters and simulation conditions

The simulated ceramic model was 0.2×1×0.4 mm, and the 3D mesh model is shown in Fig. 2. Table 2 lists the physical ceramic parameters used in the simulation. The ambient temperature is assumed to be 27 °C. The laser source acts at the

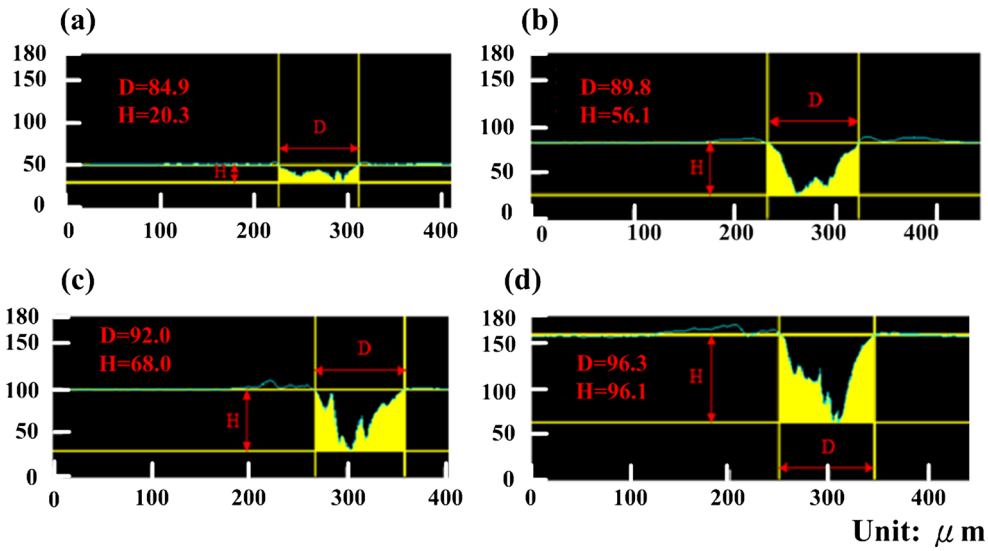

Fig. 4 Results for different laser fluences of **a** 2.55 J/cm^2, **b** 3.82 J/cm^2, **c** 5.10 J/cm^2, and **d** 6.37 J/cm^2, measured using a 3D confocal microscope

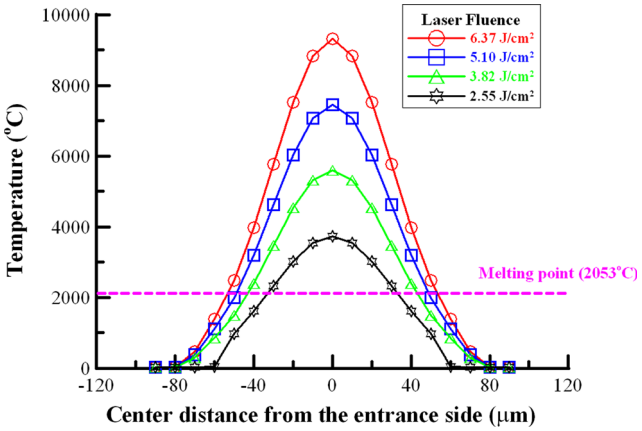

Fig. 5 Temperature distributions for the entrance hole for different laser fluences

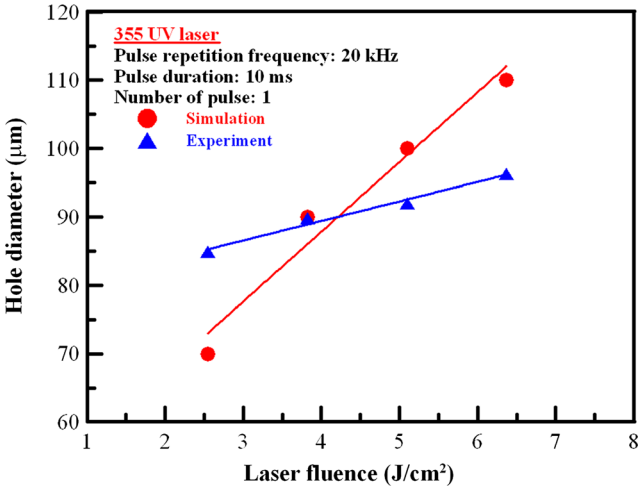

Fig. 7 Effect of laser fluence on the diameter of the drilled hole

center of the ceramic workpiece. In laser drilling, material ablation occurs through two mechanisms, melting and vaporization, which occur at 2323 and 3773 K, respectively [18]. Therefore, simulation temperatures exceeding the melting and vaporization points denote material ablation in the simulation.

4.2 Effect of laser power output on ceramic hole drilling

For experimental and simulative investigation of the influence of laser fluence on drilling, laser fluence was varied from 2.55 to 6.37 J/cm^2. The other parameters were as follows: single laser pulse, laser pulse duration of 1 ms, and laser frequency of 20 kHz. Figure 3 presents the simulation results for laser fluence values of (a) 2.55 J/cm^2, (b) 3.82 J/cm^2, (c) 5.10 J/cm^2, and (d) 6.37 J/cm^2. The simulated results reveal that an increase in laser power increases the diameter and depth of the drilled holes; the experimental results indicate that with a single laser pulse, only varying fluence cannot achieve drilling.

Figure 4 shows the 3D confocal microscopy images of holes drilled at different laser fluence values. The experimental results indicate that the drilled diameter and depth increased with increasing laser fluence; the diameter and depth ranged from 84.9 to 96.3 μm and 20.3 to 96.1 μm, respectively.

Figures 5 and 6 present the simulation results and the experimental verification of the effect of laser fluence on the diameter and depth of the holes. In Fig. 6, the *x*-axis represents the temperature of the drilled holes from its surface to its bottom. The diameters and depths of the holes drilled at different laser fluences predicted by the ANSYS finite element model were compared with the experimental values obtained under the same conditions; the results show that the maximal temperature occurs at the center and on the surface of the drilled hole. Because the laser rapidly heats the material, the melting position is around the center and the surface of the drilled hole. The simulation is consistent with the experimental results, as depicted in Figs. 7 and 8.

Fig. 6 Temperature distributions for different values of laser fluence for the drilled depth, as measured at the central position

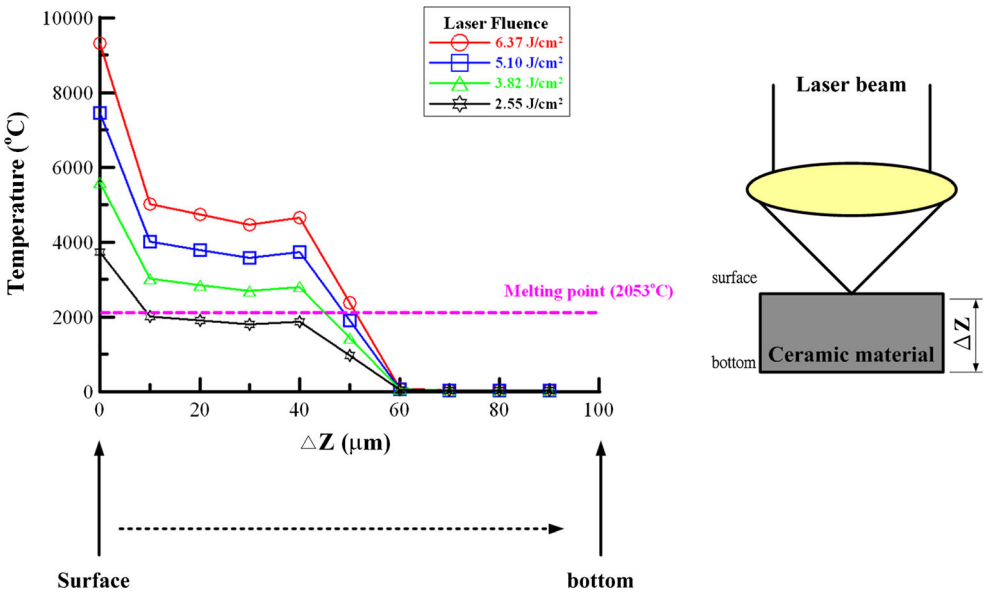

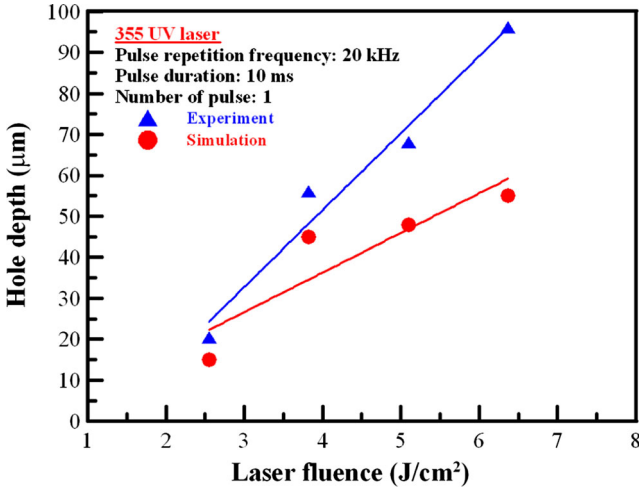

Fig. 8 Effect of the laser fluence on the drilling depth

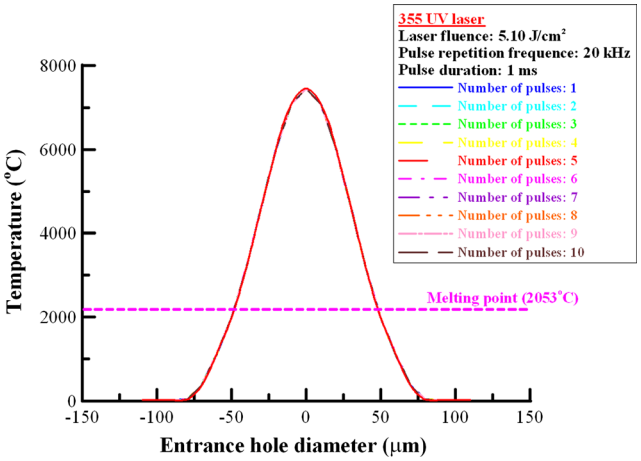

Fig. 10 Temperature distributions for the entrance holes for different numbers of pulses

Because material ablation in laser drilling of alumina ceramic involves melting and vaporization, discrepancies occur between the simulation and experimental results, as shown in Figs. 7 and 8. As shown in Fig. 7, the experimentally obtained diameters were larger than the simulated diameters at low laser fluence (i.e., 2.55 J/cm^2) because molten liquid–vapor material is ejected during drilling. This phenomenon is consistent with that proposed by Ren [8].

4.3 Effect of the number of laser pulses on ceramic hole drilling

For experimental and simulative investigation of the influence of the number of laser pulses on drilling, the number of laser pulses was varied from 1 to 10 under a laser fluence of 5.10 J/cm^2, laser pulse duration time of 1000 μs, and laser frequency of 20 kHz. Figure 9 presents the simulation results. When the number of pulses exceeded nine, the ceramic was completely drilled through. With 10 laser pulses, the diameter of the hole was enlarged, indicating that the drilled hole was tapered. This is because the focus position changes as the hole deepens; thus, laser fluence decreases and the energy spreads more widely.

Figures 10 and 11 display the temperature distribution curves for the entrance and exit of the drilled hole at a different number of laser pulses. The maximal temperature occurs at the center of the drilled holes. The simulation results indicate that the entrance diameter of the holes is larger than the exit diameter. These diameters do not change considerably when the number of pulses is varied. Figure 12 presents the optical microscopy cross-sectional view of the holes drilled with

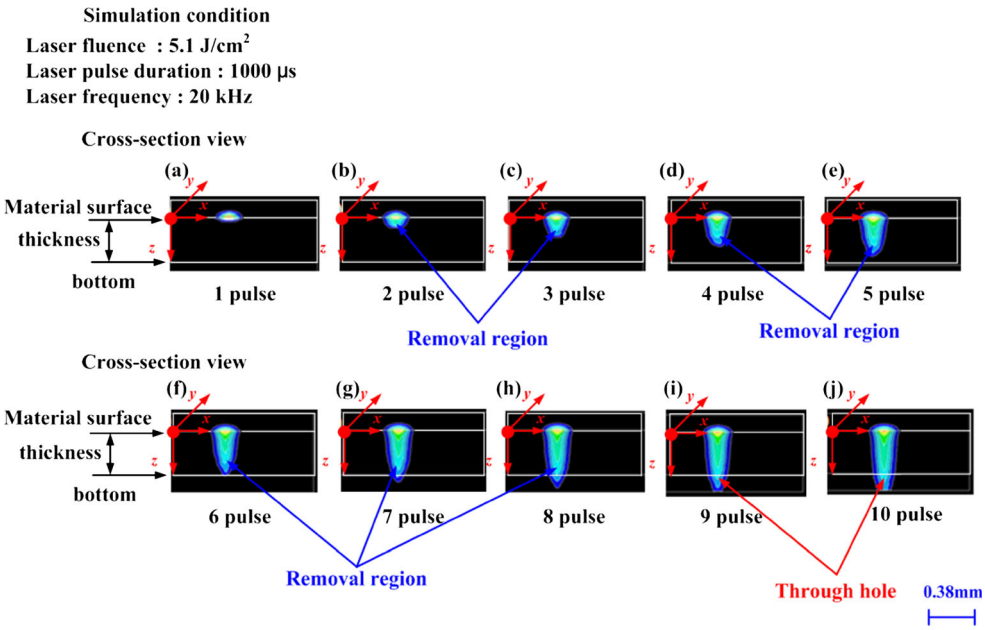

Fig. 9 Simulation images for the number of laser pulses used to drill holes in ceramic: **a** 1 pulse, **b** 2 pulses, **c** 3 pulses, **d** 4 pulses, **e** 5 pulses, **f** 6 pulses, **g** 7 pulses, **h** 8 pulses, **i** 9 pulses, and **j** 10 pulses

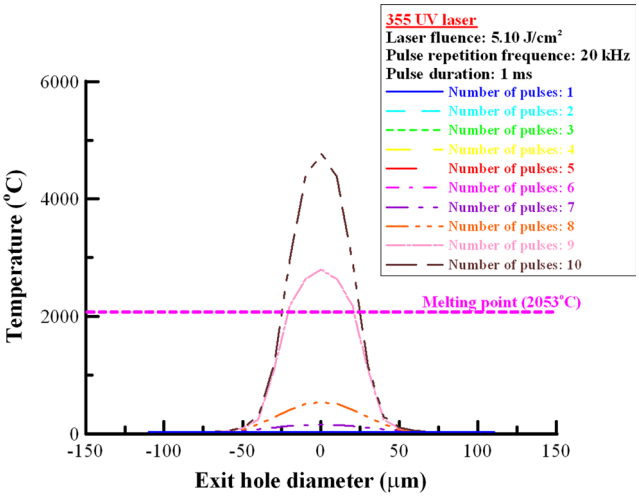

Fig. 11 Temperature distributions for the exit holes for different numbers of pulses

different numbers of pulses. The simulation and experimental results exhibit similar trends. Figure 13 shows the effect of different numbers of laser pulses on the entrance and exit diameters of the hole, and Fig. 14 shows the effect of different numbers of laser pulses on the hole depth.

Figures 10 and 11 show the temperature distribution curves for different numbers of laser pulses and for the diameter of the entrance and exit of the drilled hole. According to the temperature distribution curve, the simulation results show that the maximum temperature occurs at the center of the drilled holes. The simulation results show that the entrance diameter of the drilled holes is larger than the exit diameter. The top and bottom diameters of the drilled holes do not change significantly when the number of pulses is varied. Figure 12 shows the optical microscope cross-sectional view of the holes for different numbers of pulses. It is seen that the simulation and the experimental results show similar trends. Figure 13 shows the effect of different numbers of laser pulses on the entrance and exit diameter of the drilled hole. Figure 14 shows the effect of different numbers of laser pulses on the depth of the drilled hole.

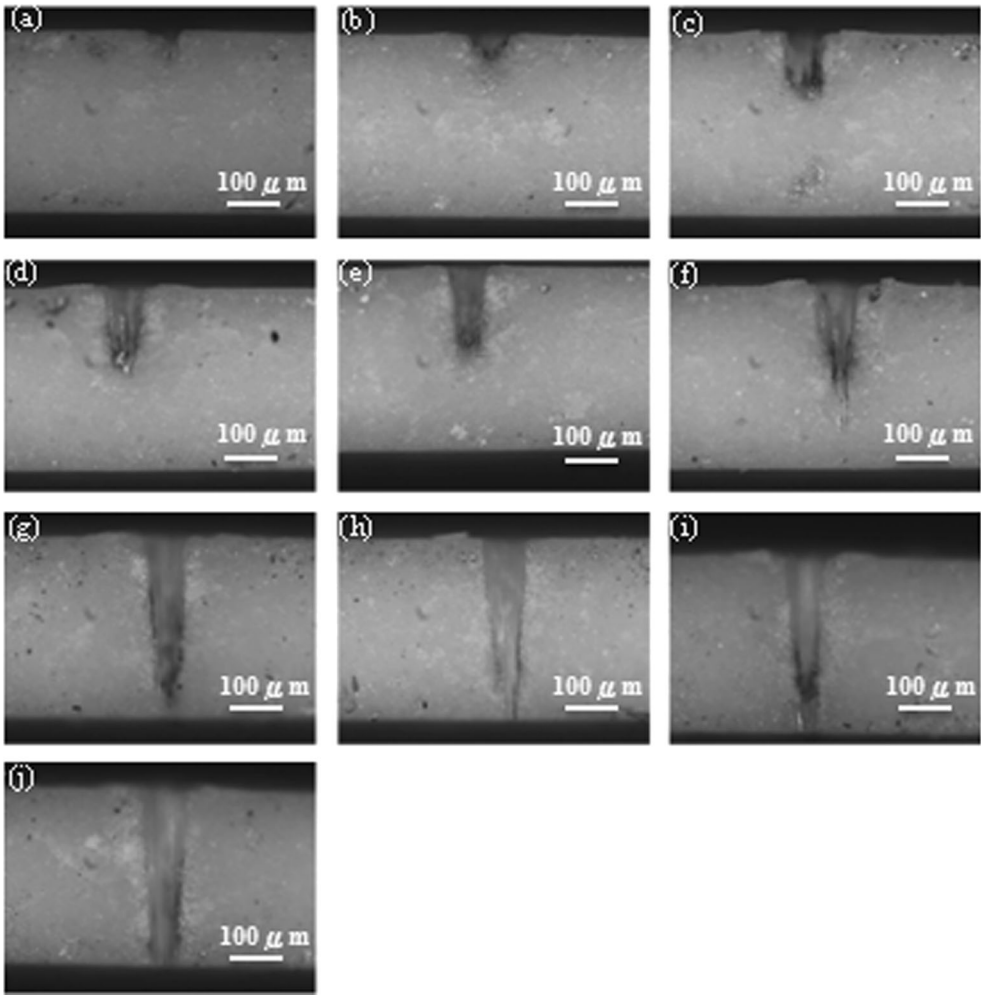

Fig. 12 Optical microscopy images for different numbers of laser pulses: **a** 1 pulse, **b** 2 pulses, **c** 3 pulses, **d** 4 pulses, **e** 5 pulses, **f** 6 pulses, **g** 7 pulses, **h** 8 pulses, **i** 9 pulses, and **j** 10 pulses

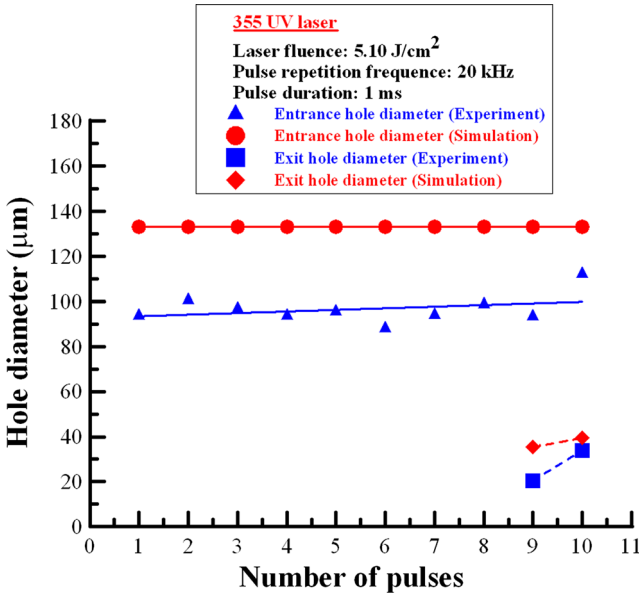

Fig. 13 Effect of different numbers of laser pulses on the entrance and exit diameter of the drilled holes

4.4 Thermal simulation and experimental results of ceramic hole drilling at different laser fluences

Figures 15 and 16 present the temperature distribution curves for the hole entrances and exits at a laser fluence of 2.55, 3.82, 5.10, and 6.37 J/cm^2. The simulation results reveal that laser fluence between 2.55 and 6.37 J/cm^2 generates temperatures that exceed the melting point of the ceramic substrate. At 2.55 J/cm^2, the maximal temperature of the ceramic bottom was 1030 °C, which cannot achieve the melting point temperature; hence, cannot obtain the through hole. An optical microscope reveals that the entrance and exit diameters increase with increasing laser fluence. The experimental and simulation results are consistent, as shown in Fig. 17.

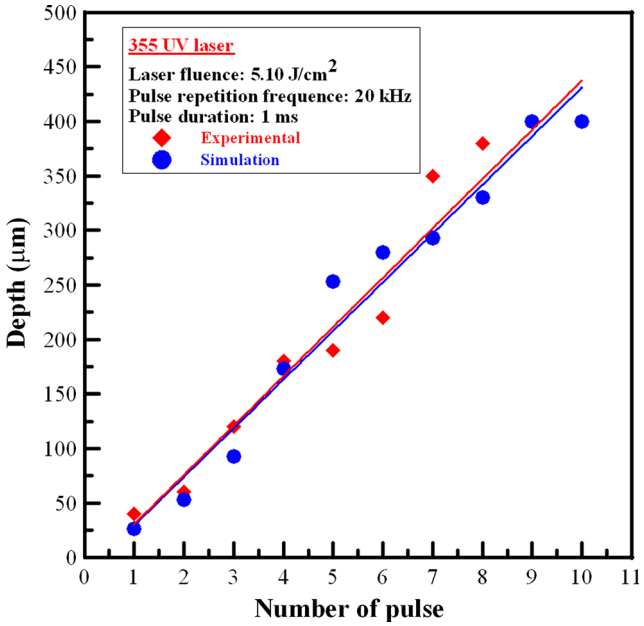

Fig. 14 Effect of different numbers of laser pulses on the depth of the drilled hole

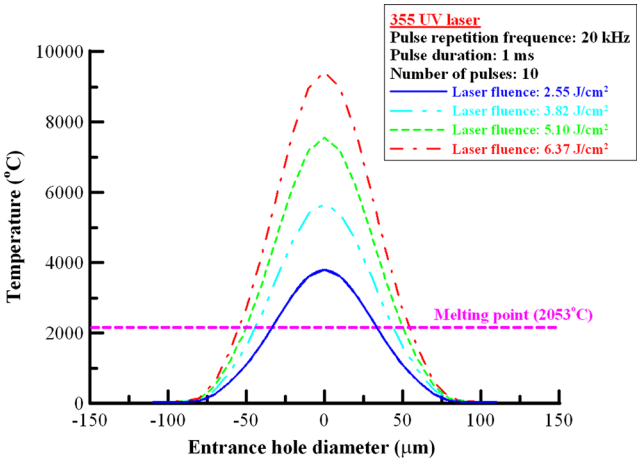

Fig. 15 Temperature distributions for the entrance holes for different values of laser fluence

4.5 Thermal simulation and experimental results of ceramic hole drilling at different pulse durations

The simulation and experimental parameters for the drilling process were as follows: 10 pulses, laser fluence of 5.10 J/cm^2, and pulse repetition frequency of 20 kHz. The laser was focused on the ceramic substrate surface. The hole diameter increases with increasing pulse duration, as shown in Figs. 18 and 19. The entrance hole diameters are larger than the exit hole diameters, resulting in an increased taper. Shorter pulses

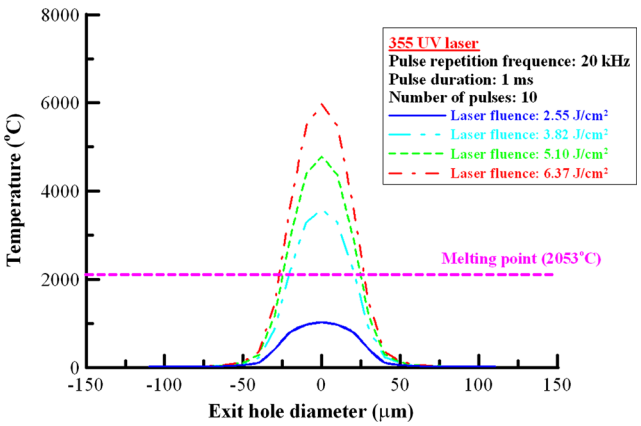

Fig. 16 Temperature distributions for the exit hole for different values of laser fluence

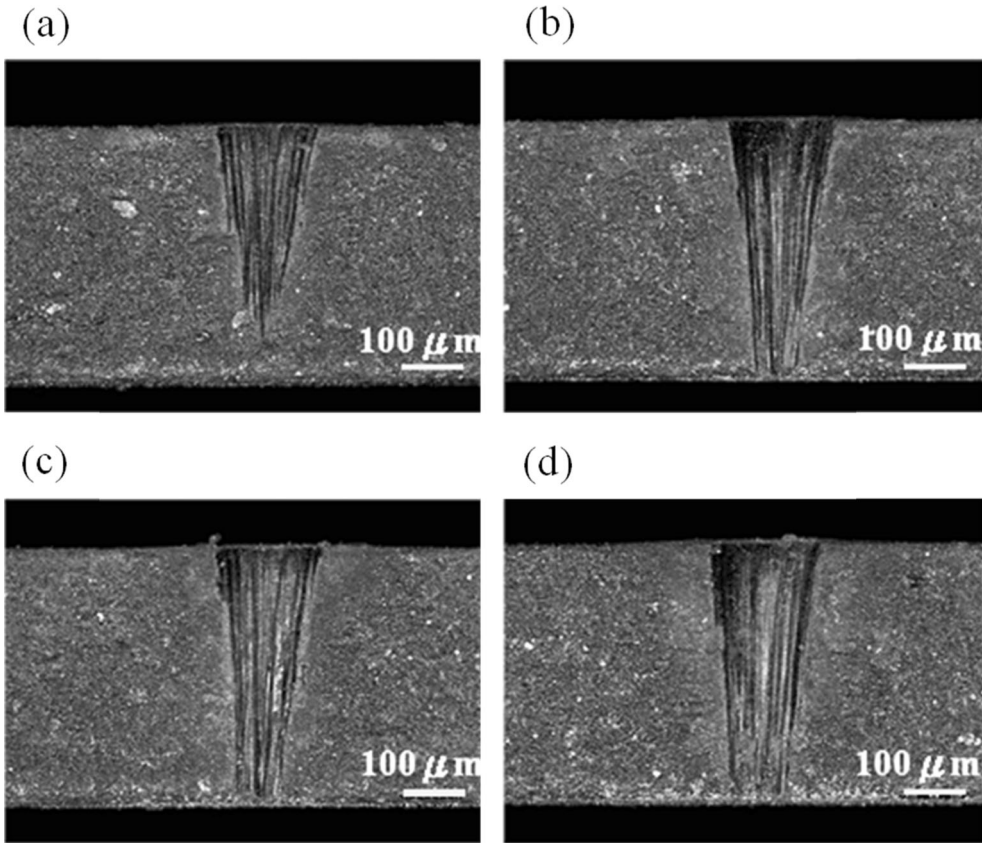

Fig. 17 Optical microscopy images for 10 pulses for different values of laser fluence: **a** 2.55 J/cm^2, **b** 3.82 J/cm^2, **c** 5.10 J/cm^2, and **d** 6.37 J/cm^2

do not considerably affect taper angle, as shown in Fig. 20. The experimental and numerical results differ slightly because shorter pulses cannot remove alumina effectively.

5 Conclusion

This paper presents theoretical and experimental methods for drilling alumina ceramic substrates using nanosecond-pulsed ultraviolet laser. A higher laser fluence and number of pulses produces larger drilling depths and diameters. However, the simulation and experimental results differ slightly because material ablation when lasing alumina ceramic entails melting and vaporization. Experimental results indicate that a laser fluence of 5.10 J/cm^2, pulse duration of 1000 μs, frequency of 20 kHz, and >9 pulses successfully drills through the alumina ceramic substrate. Pulse duration in the range of 3–8 ms yields the smallest hole taper.

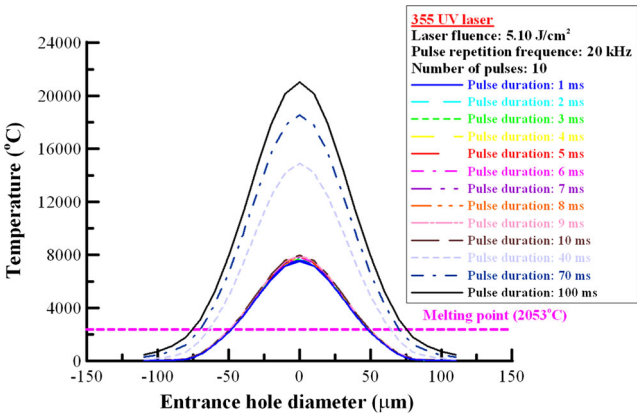

Fig. 18 Temperature distributions for the entrance hole for different laser pulse durations

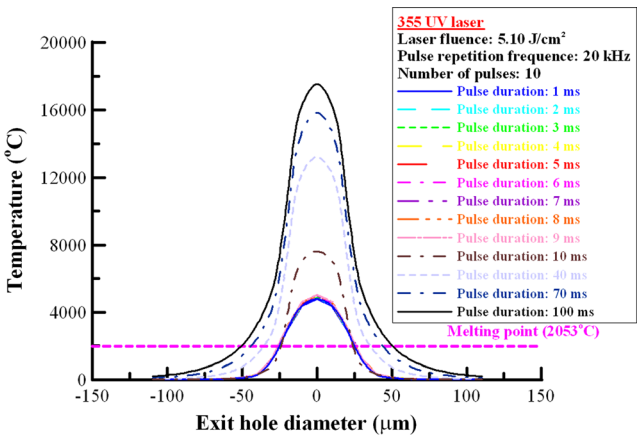

Fig. 19 Temperature distributions for the exit hole for different laser pulse durations

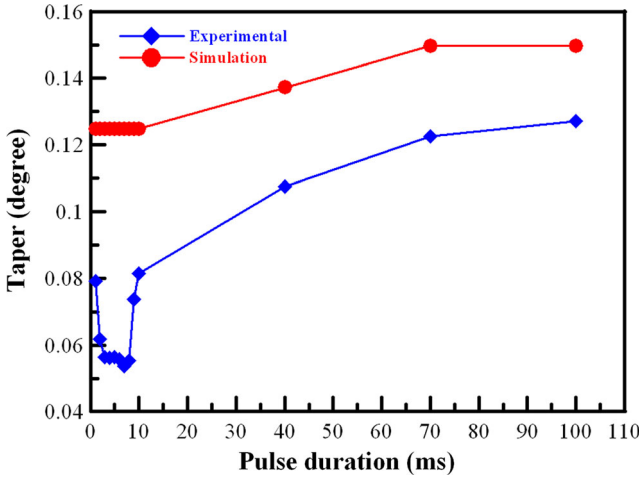

Fig. 20 Taper angles for the simulation and experiments for different laser pulse durations

References

1. Sen M, Shan HS (2005) A review of electrochemical macro-to micro-hole drilling processes. Int J Mach Tools Manuf 45:137–152
2. Bandyopadhyay S, Sarin Sundar JK, Sundararajan G, Joshi SV (2002) Geometrical features and metallurgical characteristics of Nd:YAG laser drilled holes in thick In718 and Ti-6Al-4V sheets. J Mater Process Technol 127:83–95
3. Hanon MM, Akman E, Oztoprak BG, Gunes M, Taha ZA, Hajim KI, Kacar E, Gundogdu O, Demir A (2012) Experimental and theoretical investigation of the drilling of alumina ceramic using Nd: YAG pulsed laser. Opt Laser Technol 44:913–922
4. Yang LJ, Wang Y, Tian ZG, Cai N (2010) YAG laser cutting soda-lime glass with controlled fracture and volumetric heat absorption. Int J Mach Tools Manuf 50:849–859
5. Samant AN, Paital SR, Dahotre NB (2008) Process optimization in laser surface structuring of alumina. J Mater Process Technol 203: 498–504
6. Samant AN, Dahotre NB (2009) Laser machining of structural ceramics—a review. J Eur Ceram Soc 29:969–993
7. Bharatish A, Murthy HNN, Anand B, Madhusoodana CD, Praveena GS, Krishna M (2013) Characterization of hole circularity and heat affected zone in pulsed CO_2 laser drilling of alumina ceramics. Opt Laser Technol 53:22–32
8. Ren N, Jiang L, Liu D, Lv L, Wang Q (2015) Comparison of the simulation and experimental of hole characteristics during nanosecond-pulsed laser drilling of thin titanium sheets. Int J Adv Manuf Technol 76:735–743
9. Shukla PP, Lawrence J (2012) A comparative study on the processing parameters during fiber and CO_2 laser surface treatments of silicon nitride engineering ceramic. Int J Adv Manuf Technol 59: 143–155
10. Ganguly D, Acherjee B, Kuar AS, Mitra S (2012) Hole characteristics optimization in Nd:YAG laser micro-drilling of zirconium oxide by grey relation analysis. Int J Adv Manuf Technol 61: 1255–1262
11. Kibria G, Doloi B, Bhattacharyya B (2015) Investigation and analysis on pulsed Nd:YAG laser micro-turning process of aluminium oxide (Al_2O_3) ceramic at various laser defocusing conditions. Int J Adv Manuf Technol 76:17–27
12. Adelmann B, Hellmann R (2015) Rapid micro hole laser drilling in ceramic substrates using single mode fiber laser. J Mater Process Technol 221:80–86
13. Mishra S, Yadava V (2013) Modeling and optimization of laser beam percussion drilling of thin aluminum sheet. Opt Laser Technol 48:461–474
14. Sowdari D, Majumdar P (2010) Finite element analysis of laser irradiated metal heating and melting processes. Opt Laser Technol 42:855–865
15. Zhang Y, Li S, Chen G (2013) Experimental observation and simulation of keyhole dynamics during laser drilling. Opt Laser Technol 48:405–414
16. Collins J, Gremaud P (2011) A simple model for laser drilling. Math Comput Simul 81:1541–1552
17. Chen BC, TsaiYH HCY (2013) Parametric effects on femtosecond laser ablation of Al_2O_3 ceramics. Ceram Int 39:341–344
18. McColm IJ (1983) Ceramics science for materials technologists. LH, New York